

Spectroscopic and Solution Properties of Phenoxyphosphazene Random Copolymers Containing Optically Active Binaphthoxy Groups

Gabino A. Carriedo,* Francisco J. García Alonso, Paloma Gómez Elipe, and José L. García-Alvarez

Departamento de Química Orgánica e Inorgánica, Facultad de Química, Universidad de Oviedo, Oviedo 33071, Spain

M. Pilar Tarazona,* M. Teresa Rodríguez, and Enrique Saiz

Departamento de Química Física, Facultad de Química, Universidad de Alcalá de Henares, 28871 Alcalá de Henares, Spain

Jesús T. Vázquez* and Juan I. Padrón

Instituto Unversitario de Bio-Orgánica "Antonio González", Universidad de La laguna, Tenerife, Spain

Received November 12, 1999; Revised Manuscript Received February 14, 2000

ABSTRACT: The reaction of a mixture of $[\text{NPCl}_2]_n$ and Cs_2CO_3 first with (*R*)-(+)-1,1'-binaphthyl-2,2'-diol ($\text{HO}-\text{C}_{10}\text{H}_6-\text{C}_{10}\text{H}_6-\text{OH}$) (binaphthol) and subsequently with phenol ($\text{HO}-\text{C}_6\text{H}_5$) in refluxing 1,4-dioxane gave the series of the optically active random copolymers $\{[\text{NP}(\text{O}_2\text{C}_{20}\text{H}_{12})_x][\text{NP}(\text{OC}_6\text{H}_5)_2]_{1-x}\}_n$ (**2**). Absolute molecular weight distributions and radius of gyration have been determined by size exclusion chromatography, using simultaneously multiangle light scattering and differential refractive index detectors. The dependence of the dimensions of the polymers on the molecular weight through the corresponding scaling laws is studied. In addition, a stereochemical study of homopolymers $[\text{NP}(\text{O}_2\text{C}_{20}\text{H}_{12})]_n$ **1** and copolymers **2** based on the CD exciton chirality method is also included. The reaction of the partially substituted polymer $[\text{NP}(\text{R}-\text{O}_2\text{C}_{20}\text{H}_{12})_{0.4}(\text{Cl}_2)_{0.6}]_n$ with the stoichiometric amount of racemic binaphthol, or with a large excess of the latter, in the presence of Cs_2CO_3 gave the same polymer $[\text{NP}(\text{R}-\text{O}_2\text{C}_{20}\text{H}_{12})_{0.4}(\text{rac}-\text{O}_2\text{C}_{20}\text{H}_{12})_{0.4}]_n$ [(−)-**3**] irrespective of the amount of racemic binaphthol used, showing no enantiomeric induction by the *R*-binaphthoxy units already present in the polymer.

Introduction

Polyphosphazenes are a very important class of inorganic polymers that deserve a great deal of interest due to the variety of properties, chemical and mechanical, that can be easily incorporated into them.¹ Earlier,² we reported the synthesis of the high molecular weight chiral polymeric phosphazenes $[\text{NP}(\text{O}_2\text{C}_{20}\text{H}_{12})]_n$ (**1**) (Chart 1) directly from polydichlorophosphazene $[\text{NPCl}_2]_n$ and 1,1'-binaphthyl-2,2'-diol ($\text{HO}-\text{C}_{10}\text{H}_6-\text{C}_{10}\text{H}_6-\text{OH}$) (binaphthol). Previously, Sulkowski et al.³ had reported the preparation of various aryloxyphosphazene random copolymers of low molecular weight having some racemic spirobinaphthalenedioxy groups, which exhibit high thermal stability.

The presence of binaphthyl units in a polymer is very interesting.⁴ Some recent uses include the making of materials for host–guest interactions useful in enantiomeric separations,⁵ catalysis,⁶ or the incorporation of chirality in LB films.⁷

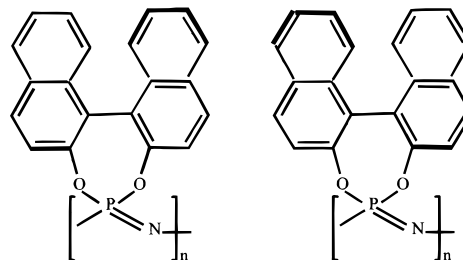
To extend the range of polyphosphazene having optically active spirobinaphthoxy units and to better understand their solution properties, we have synthesized the random copolymers of general formulas $\{[\text{NP}(\text{O}_2\text{C}_{20}\text{H}_{12})_x][\text{NP}(\text{OC}_6\text{H}_5)_2]_{1-x}\}_n$ (**2**) and studied them by light scattering techniques and circular dichroism.

Experimental Section

Materials. All the reactions were carried out under dry nitrogen.

* Corresponding authors. E-Mail: gac@sauro.n. quimica.uniovi.es; gfmptl@alcala.es; or jtruvaz@ull.es.

Chart 1



(+)-1 and (−)-1

Cs_2CO_3 was dried at 140 °C prior to use. 1,4-Dioxane was distilled from Na in the presence of benzophenone. Petroleum ether refers to that fraction with boiling point in the range 60–65 °C. The hexachlorocyclotriphosphazene $[\text{N}_3\text{P}_3\text{Cl}_6]$ (Fluka) was purified from hot petroleum ether and dried in a vacuum. The starting polymer $[\text{NPCl}_2]_n$ was prepared by the polymerization reaction in solution described by Magill et al.⁸ The (*R*)-(+)-binaphthol⁹ was prepared as described in the literature. For the reactions we used a product having $[\alpha]_D$ of +35.3 (at $c = 1$ in THF). UV (CH_3CN): λ_{max} (ϵ , $\text{L cm}^{-1} \text{mol}^{-1}$) 338 (6.500), 278 (7.500), 229 nm (75.000). CD (CH_3CN): λ_{ext} ($\Delta\epsilon$) 319 (7.3), 234 (−208.7), 228 (0.0), 222 nm (152.3).

Measurements. The IR spectra were recorded with Perkin-Elmer Paragon 1000 spectrometer. NMR spectra were recorded on Bruker AC-200 and AC-300 instruments, using CDCl_3 as solvent unless otherwise stated. ^1H and $^{13}\text{C}\{^1\text{H}\}$ NMR are given in δ relative to TMS. $^{31}\text{P}\{^1\text{H}\}$ NMR are given in δ relative to external 85% aqueous H_3PO_4 . Coupling constants are in hertz. C, H, and N analyses were performed with a Perkin-Elmer 2400 microanalyzer. The chlorine analy-

Table 1. Experimental Data for the Polymer Synthesis

polymer	W_{PCL} [g (mmol)] ^a	W_{Bin} [g (mmol)] ^a	W_{Ph} [g (mmol)] ^a	W_{Cs} [g (mmol)] ^a	V (mL) ^a	t_1 (h) ^a	t_2 (h) ^a	yield [g (%)]
2a	2.04 (17.6)	0.50 (1.76)	3.3 (35.06)	17.20 (52.8)	120	2.5	36.5	0.76 (18)
2b	2.02 (17.5)	1.0 (3.49)	3.0 (31.9)	17.07 (52.4)	150	3.5	21.5	1.40 (32)
2c	1.90 (16.4)	1.88 (6.56)	2.15 (22.9)	16.03 (49.2)	150	7	32.25	1.47 (34.1)
2d	1.67 (14.4)	2.47 (8.63)	1.20 (12.7)	14.04 (43.1)	100	10	23.5	3.33 (83.8)
2e	0.80 (6.85)	1.58 (5.51)	0.49 (4.76)	6.74 (20.7)	90	12	14	1.46 (70.7)

^a For the meaning of the different abbreviations used in the Table 1, see the experimental part in the text.

Table 2. Analytical, Molecular Weight, and Specific Rotation for the Polymers 2

polymer	x^a	% C [calc (found)]	% H [calc (found)]	% N [calc (found)]	% Cl	M_w (M_w/M_n) ^b	α^{20}_D ^c
2a	0.08	63.5 (62.9)	4.28 (3.61)	5.86 (5.90)	0.06	950 000 (1.9)	−59
2b	0.17	64.7 (64.6)	4.20 (3.70)	5.65 (5.72)	0.05	930 000 (4.3)	−110
2c	0.32	66.6 (65.1)	4.08 (3.83)	5.33 (5.15)	0.09	1 160 000 (4.2)	−135
2d	0.42	67.7 (65.3)	4.01 (3.70)	5.09 (5.29)	0.04	1 200 000 (2.6)	−136
2e	0.70	70.5 (70.2)	3.83 (3.56)	4.67 (4.93)	0.04	1 000 000 (4.6)	−149

^a By integration of the two signals in the ³¹P NMR measured at room temperature in CHCl₃ or DMSO-*d*₆ at 120 °C. ^b Molecular weight determined by GPC. ^c Measured in CHCl₃ at $c = 1$.

ses were performed by Galbraith Laboratories. GPC were measured with a Perkin-Elmer equipment with a model LC 250 pump, a model LC 290 UV, and a model LC 30 refractive index detector. The samples were eluted with a 0.1 wt % solution of tetra-*n*-butylammonium bromide in THF through Perkin-Elmer PLGel (Guard, 10⁵, 10⁴, and 10³ Å) at 30 °C. Approximate molecular weight calibrations were obtained using narrow molecular weight distribution polystyrene standards. The absolute molecular weight distributions and radii of gyration were determined by size exclusion chromatography (SEC) combined with multiangle laser light scattering, MALLS. A Waters Associates differential refractive index detector model 410 was used as concentration detector, and a Dawn-DSP-F laser photometer from Wyatt Technology Corp. was the mass and size detector used. A model 510 pump, a U6K injector (Waters Associates), and two columns PLgel mixed B (Polymer Laboratories) in series completed the equipment. The eluent was the same as above. The Dawn photometer was calibrated with spectrometric grade toluene freshly distilled from sodium and benzophenone, and the normalization of the detectors was performed with standard monodisperse polystyrene of low molecular weight that did not show angular dependence on the light scattering signal. Standard monodisperse polystyrene was also used to determine the interdetector volume. The refractive index increments for the polymers were measured with a Brice-Phoenix differential refractometer at 436 and 546 nm and extrapolated to 632 nm using the Cauchy relationship.

CD spectra were recorded in the range 400–200 nm and by using a 10 mm cell on a JASCO J-600 spectropolarimeter. Because of the low solubility of the polymers in CH₃CN, their CD samples were prepared by dissolving the accurately weighted compound in 25 mL calibrated flasks with 5 mL of THF and then with CH₃CN to obtain solutions containing 0.2 mg/mL. Then measured volumes of these solutions (100 μ L) were diluted in 10 mL calibrated flasks with CH₃CN.

T_g values were measured with a Mettler DSC 300 differential scanning calorimeter equipped with a TA 1100 computer at 10 °C/min. Thermal gravimetric analysis were performed on a Mettler TA 4000 instrument. The polymer samples were heated at a rate of 10 °C/min from ambient temperature to 800 °C under constant flow of nitrogen. The specific optical rotation $[\alpha]_D$ was measured with a Perkin-Elmer 343 polarimeter, near 25 °C in CHCl₃ (or THF) solution at $c = 1$ unless otherwise stated, checking every time that the value for (−)-cinchonidine in ethanol was in the range 106 \pm 3° at $c = 1.5$.

Synthesis of the Polyphosphazenes. [NP(O₂C₂₀H₁₂)]_n [(−)-1]. See ref 2. UV (CH₃CN): λ_{max} 326, 306, 231 nm. CD (CH₃CN): λ_{ext} ($\Delta\epsilon_{\text{res}}$) 303 (7.5), 263 (−25.0), 243 (11.2), 229 (−190.8), 213 nm (77.6). CD ($c = 1 \times 10^{-3}$ mg/mL CH₃CN): λ_{ext} (θ , mdeg) 325 (0.7), 263 (−2.5), 243 (1.1), 229 (−19.1), 213 nm (7.8).

[NP(O₂C₂₀H₁₂)]_n [(+)-1]. See ref 2. UV (CH₃CN): λ_{max} 326, 306, 231 nm. CD (CH₃CN): λ_{ext} ($\Delta\epsilon_{\text{res}}$) 303 (−11.2), 263 (19.6), 243 (−16.2), 228 (176.5), 212 nm (−79.9).

{[NP(O₂C₂₀H₁₂)]_x[NP(OC₆H₅)₂]_{1−x}}]_n [(−)-2]. [$x = 0.08$ (**2a**), 0.17 (**2b**), 0.32 (**2c**), 0.42 (**2d**), 0.70 (**2e**)].

All the polymers were prepared by the same procedure using the amounts of the reagents and reaction times shown in Table 1.

To a solution of [NPCL₂]_n [W_{PCL} g, (mmol)] in dioxane (V mL) (+)-(HO)₂(C₂₀H₁₂) ($[\alpha]_D = +35.3$) [W_{Bin} g, (mmol)] and Cs₂CO₃ [W_{Cs} g, (mmol)] were added, and the mixture was refluxed for t_1 hours with vigorous mechanical stirring. To the mixture, phenol (HOC₆H₅) [W_{Ph} g, (mmol)] was added, and refluxing was continued for t_2 hours. The resulting mixture was poured into water to give a white solid that was extracted overnight with THF (0.5 L) and filtered to give a transparent solution. This was concentrated at reduced pressure to a viscous liquid that was poured slowly into water. The resulting solid was similarly reprecipitated from THF/2-propanol and THF/petroleum ether. The resulting white product was dried first in a vacuum at room temperature and then at 70 °C for 2–10 days to give the white polymers [(−)-2]. Yield (g, %).

¹H NMR (CDCl₃): 10–5 very broad with a maxima at ca. 7.1 and 6.5 (m, aromatic rings). Measured in DMSO-*d*₆ at 393 K, the protons of the aromatic rings give a multiplet with peaks at 6.76, 6.87, 6.98, 7.2, 7.59, 7.69. ¹³C NMR (CDCl₃): 148, 132, 131, 130, 128, 127, 126, 125, 122, 121 (O₂C₁₂H₂₀); 152, 129, 124, 121(OC₆H₅). ³¹P{¹H} NMR (CDCl₃): −2 to −6 (broad and complex multiplet) [NP(O₂C₁₂H₂₀)]; −21 to −24 (broad and complex multiplet) [NP(OC₆H₅)₂]. The integration of both signals gave the values of x given in Table 2. Similar results were obtained measuring the spectra in DMSO-*d*₆ at 393 K.

Anal. Calcd NPO₂C_{12+8x}H_{10+2x} (see Table 2). M_w (GPC), M_w/M_n , $[\alpha]_D^{30}$ (see Table 2).

Compound **2a**. UV (CH₃CN): λ_{max} 312, 236, 213, 203 nm. CD ($c = 1 \times 10^{-3}$ mg/mL CH₃CN): λ_{ext} (θ , mdeg) 351 (−0.2), 263 (−1.5), 230 (−4.4), 207 nm (−1.4).

Compound **2b**. UV (CH₃CN): λ_{max} 312, 226, 201 nm. CD ($c = 1 \times 10^{-3}$ mg/mL CH₃CN): λ_{ext} (θ , mdeg) 262 (−1.2), 231 (−6.5), 216 nm (1.6).

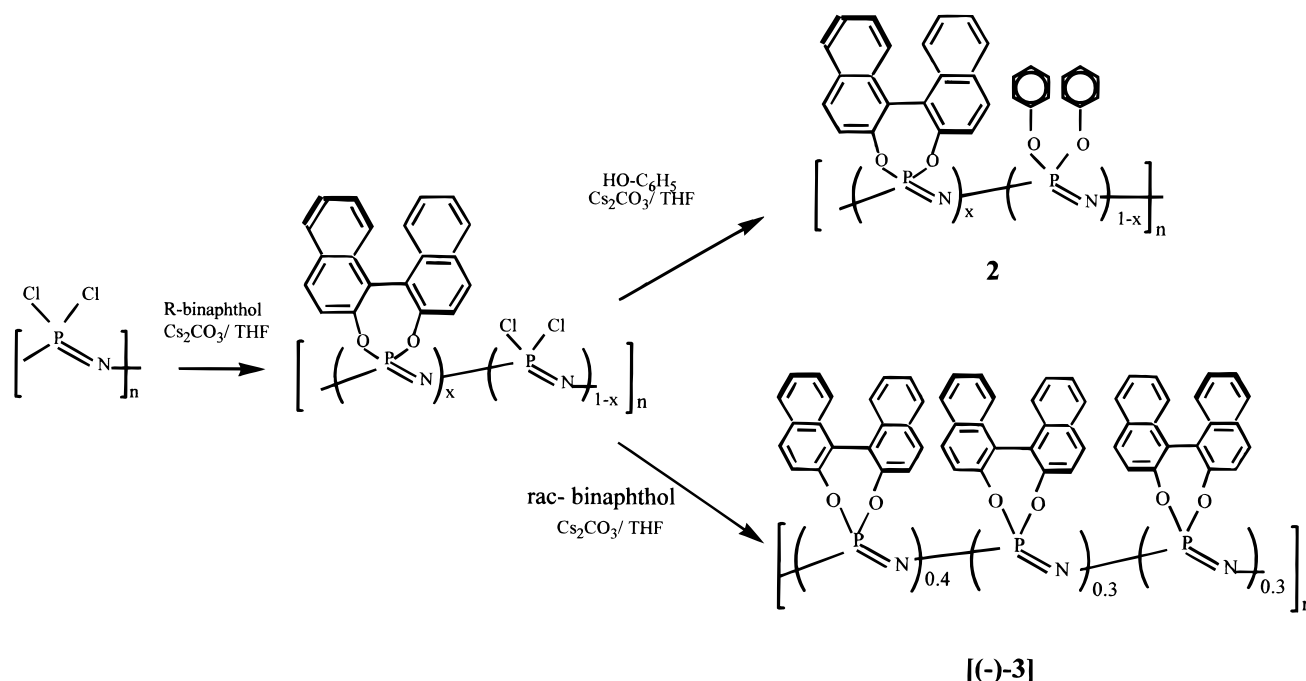
Compound **2c**. UV (CH₃CN): λ_{max} 312, 225, 203 nm. CD ($c = 1 \times 10^{-3}$ mg/mL CH₃CN): λ_{ext} (θ , mdeg) 325 (0.1), 264 (−2.0), 230 (−10.9), 214 nm (3.3).

Compound **2d**. UV (CH₃CN): λ_{max} 226, 202 nm. CD ($c = 1 \times 10^{-3}$ mg/mL CH₃CN): λ_{ext} (θ , mdeg) 325 (0.5), 262 (−1.4), 229 (−10.4), 212 nm (4.6).

Compound **2e**. UV (CH₃CN): λ_{max} 226, 202 nm. CD ($c = 1 \times 10^{-3}$ mg/mL CH₃CN): λ_{ext} (θ , mdeg) 324 (0.6), 262 (−2.4), 244 (0.2), 229 (−16.0), 212 nm (7.2).

[NP(R−O₂C₂₀H₁₂)_{0.4}(*rac*-O₂C₂₀H₁₂)_{0.6})]_n [(−)-3]. To a solution of [NPCL₂]_n (1.184 g, 10.22 mmol) in dioxane (100 mL) were added (+)-(HO)₂(C₂₀H₁₂) ($[\alpha]_D = +35.3$) (1.171 g, 4.09 mmol) and Cs₂CO₃ (10 g, 30.66 mmol), and the mixture was refluxed

Scheme 1



for 6.75 h with vigorous mechanical stirring. To the mixture racemic binaphthol ($\text{HO})_2(\text{C}_{20}\text{H}_{12})$ (1.84 g, 6.43 mmol) was added, and refluxing was continued for 14.5 h. The resulting mixture was poured into water to give a white solid that was extracted overnight with THF (0.5 L) and filtered to give a transparent solution. This was concentrated at reduced pressure to a viscous liquid that was poured into water. The resulting solid was similarly reprecipitated from THF/2-propanol and THF/petroleum ether. The resulting white product was predried first in a vacuum at room temperature and then at 70 °C for 7 days to give the white polymer **[(-)-3]**. Yield: 1.3 g, 38.6%.

The ^1H NMR showed that the hydrocarbons retained (calculated as hexanes) were of the order of 1 wt %.

Anal. Calcd for $\text{C}_{20}\text{H}_{12}\text{O}_2\text{NP}$: C, 73.0; H, 3.67; N, 4.25. Found: C, 71.0; H, 3.50; N, 4.00. $M_w(\text{GPC})$: 780 000, M_w/M_n = 7.1. $[\alpha]_D^{30} = -50^\circ$ in CHCl_3 .

The same compound resulted using the stoichiometric amount of racemic binaphthol. $M_w(\text{GPC})$: 880 000, M_w/M_n = 5.9. $[\alpha]_D^{30} = -57^\circ$ in CHCl_3 .

Compound (+)-4: See ref 2. UV (CH_3CN): λ_{max} 302 (20.000), 234 (85.000), 217 nm (190.000). CD (CH_3CN) λ_{ext} ($\Delta\epsilon$) 323 (-19.7), 290 (-39.0), 259 (22.7), 237 (-137.4), 225 (587.1), 215 nm (-459.8).

Results and Discussion

The reaction in refluxing dioxane of $[\text{NPCl}_2]_n$, prepared by Magill's method,⁸ first with (+)-($\text{HO})_2(\text{C}_{20}\text{H}_{12})$ ($[\alpha]_D = +35.3$) in THF and subsequently with an excess of phenol to complete the chlorine substitution (see Experimental Section and Table 1), gave the random copolymers $\{[\text{NP}(\text{O}_2\text{C}_{20}\text{H}_{12})_x[\text{NP}(\text{OC}_6\text{H}_5)_2]_{1-x}]\}_n$ (**2**) [$x = 0.08$ (**2a**), 0.17 (**2b**), 0.32 (**2c**), 0.42 (**2d**), 0.70 (**2e**)] (Scheme 1). The yields varied from moderate to very good. The observed x values were close but not identical to those intended, which is attributable to the difficulty of following by ^{31}P NMR the advance of the first substitution process in dioxane. In fact, on repeating the preparations, the values of x found show oscillations within 10% of those given above.

All the analytical (Table 2) and spectroscopic data (Experimental Section) for the polymers **2** were in accord with their proposed structure, and in all cases

the residual chlorine was below 0.1%. The molecular weights as determined by GPC with polystyrene standards were of the order of 10^6 (Table 2), showing slight variations (ca. 10%) on repeating the preparations.

Significantly, the ^{31}P NMR showed two broad and complex signals, one centered around -5 ppm and the other -22 ppm, that varied in shape and intensity with the value of x and that allowed a measure of this value in each polymer. The spectra, which were better resolved in $\text{DMSO}-d_6$ at 120 °C (Figure 1), showed a pseudotriplet in the region of -5 ppm whose variation of intensity with x suggested that it might correspond to the $[\text{NP}(\text{O}_2\text{C}_{20}\text{H}_{12})]$ units being in the middle of two $[\text{NP}(\text{OC}_6\text{H}_5)_2]$ units.

The increasing content of binaphthoxy units was also noted in the intensity of the corresponding peaks in the ^{13}C NMR spectra, better observed in $\text{DMSO}-d_6$ at 120 °C.

On the other hand, the IR spectra, in Nujol mull, showed no signals for terminal HO groups, showing that there are no (or very few) "monodentated" binaphthoxy units in the polymers.

The presence of chiral binaphthoxy units in the partially substituted intermediate copolymer $\{[\text{NP}(\text{O}_2\text{C}_{20}\text{H}_{12})_x[\text{NP}(\text{Cl})_2]_{1-x}]\}_n$ suggested the possibility for chirality induction in their reactions with more binaphthol. However, we observed that the reaction of the polymer $\{[\text{NP}(\text{R}-\text{O}_2\text{C}_{20}\text{H}_{12})_{0.4}[\text{NP}(\text{Cl})_2]_{0.6}]\}_n$ with racemic binaphthol in the presence of Cs_2CO_3 (Scheme 1) gave almost identical polymers $[\text{NP}(\text{R}-\text{O}_2\text{C}_{20}\text{H}_{12})_{0.4}(\text{rac}-\text{O}_2\text{C}_{20}\text{H}_{12})_{0.6}]\}_n$ **[(-)-3]**, analogous to **1**, having $[\alpha]_D^{30}$ of ca. -50 in CHCl_3 , either using the stoichiometric amount of racemic binaphthol (to force the entering of both enantiomeric binaphthoxy units) or a very large excess of the latter (to ensure that enough *R*-isomer was available to complete the chlorine substitution alone).

Not unexpectedly,^{2,3} the binaphthoxy polyphosphazenes **2** were thermally very stable. The TGA curves showed a quick decomposition only at temperatures close to 500 °C, which increase very little with x [493

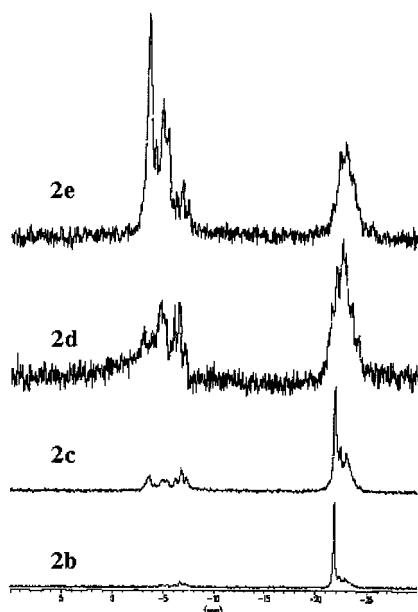


Figure 1. ^{31}P NMR spectra of polymers **2b**–**2e** in $\text{DMSO}-d_6$ at $120\text{ }^\circ\text{C}$.

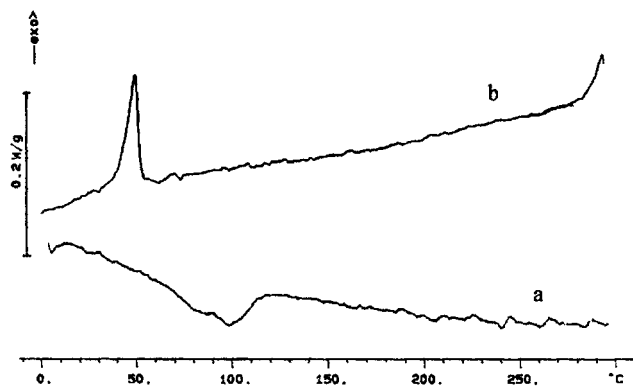


Figure 2. DSC curves for polymer **2a** from 0 to $300\text{ }^\circ\text{C}$ at $10\text{ }^\circ\text{C min}^{-1}$: (a) third heating cycle; (b) third cooling cycle.

(0.08), 484 (0.17), 484 (0.32), 491 (0.42), 528 (0.7). For the homopolymer **1**, the observed value was $540\text{ }^\circ\text{C}$.² The residue at $800\text{ }^\circ\text{C}$ varied from 40 to 50% with increasing x . Even though the weight loss observed in the TGA curves may depend on the scan rate of the measurements, this behavior resembles that of other important materials that exhibit a large thermal stability.¹⁰ It should be taking into account, however, that, as observed for **1**, the heating reduces the M_w by a degradation process of the polymeric chains not resulting in weight loss.²

In the DSC curves corresponding to polymers **2** it was not possible to unambiguously identify a glass transition that should be intermediate between that of the two homopolymers $[\text{NP}(\text{OC}_5\text{H}_6)_2]_n$ (T_g at $-8\text{ }^\circ\text{C}$)¹¹ and $[\text{NP}(\text{O}_2\text{C}_{20}\text{H}_{12})_2]_n$ (**1**) (not detected below $200\text{ }^\circ\text{C}$).² Only in the case of **2a**, having 8% of binaphthoxy units, did the curve (Figure 2) suggest a glass transition near $65\text{ }^\circ\text{C}$ and an endothermic peak close to $100\text{ }^\circ\text{C}$. On the cooling cycle a sharp exothermic peak centered at $52\text{ }^\circ\text{C}$ ($\Delta H = 8.4\text{ J g}^{-1}$) evidenced the crystallization of the polymer. By comparison with other phenoxyphosphazenes random copolymers,¹² it seems that above $100\text{ }^\circ\text{C}$ polymer **2a** forms a mesophase. A more detailed study of those aspects is underway.

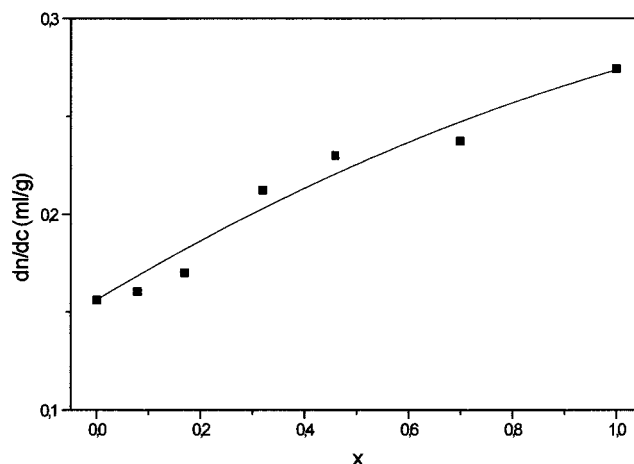


Figure 3. Specific refractive index increments, dn/dc , in THF solution, versus the number of binaphthoxy units for polymers **1**, **2a**, **2b**, **2c**, **2d**, **2e**, and poly(diphenoxyphosphazene).

The specific refractive index increments, dn/dc , in THF solution versus the number of binaphthoxy units (x) for polymers **2** together with the corresponding values of the homopolymer **1** ($x = 1$) and poly(diphenoxyphosphazene)¹³ ($x = 0$) are presented in Figure 3. The solid line in the same figure represents the calculated values assuming that the refractive index increment is an additive function of the composition of the polymer expressed in terms of the weight fractions.¹⁴ The coincidence of the experimental data and theoretical curve is very good.

The use of a multiangle light scattering detector enables the evaluation of the weight-averaged molecular weight and the mean-square radius of gyration $\langle s^2 \rangle$ for each slice across a sample peak of the size exclusion chromatogram. Thus, absolute calibration curves for SEC, i.e., molecular weight versus exclusion volume curves, and the dependence of molecular dimensions on molecular weight, i.e., $\langle s^2 \rangle^{1/2}$ versus M curves, are obtained. Figure 4 shows the molecular weight versus elution volume plots for homopolymer **1** and polymers **2**. The signal from the differential refractive index detector (DRI), proportional to the polymer concentration, has also been plotted. The combined measurements of molecular weight, obtained with the MALLS detector, and concentration, obtained with a differential refractive index detector, DRI, for each elution volume, allows to determine the absolute molecular weight distributions for the polymer samples.¹⁵ Mean values of molecular weights, polydispersities, and the corresponding standard deviations, obtained using ASTRA software, are listed in Table 3.

As can be seen in Figure 4, the polymers exhibit the same behavior, i.e., similar absolute SEC calibration curves, with the exception of polymer **2d** for which a rather different curve is obtained. Thus, any given value of elution volume v_e represent a much lower molecular weight in the case of the **2d** polymer than in the rest of the samples studied here. It is worth pointing out the significant differences between relative and absolute molecular weights for these polymers. For instance, the DRI signal for polymer **2d** (dotted line in Figure 4) appears in the same range, or even at lower elution volumes, than the equivalent signals for the other polymers. Thus, the relative molecular weight calculated with polystyrene standards for this sample is similar

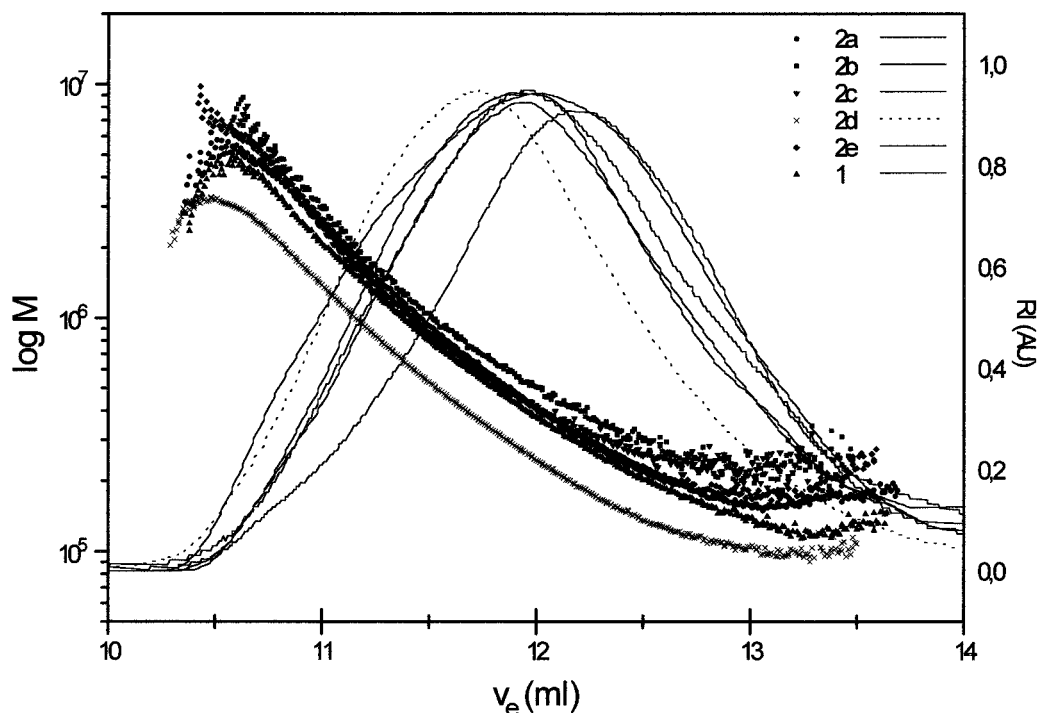


Figure 4. Logarithm of molecular weight versus elution volume for polymers **1**, **2a**, **2b**, **2c**, **2d**, and **2e**. The corresponding DRI (differential refractive index) signals are also shown.

Table 3. Averaged Molecular Weights, Polydispersities, Root-Mean-Square Radii of Gyration, and Scaling Parameters of Polyphosphazenes

polymer	$10^{-5}M_n$ (g/mol)	$10^{-5}M_w$ (g/mol)	$10^{-6}M_z$ (g/mol)	M_w/M_n	$\langle s^2 \rangle_z^{1/2}$ (nm)	q
1	2.89 ± 0.04	6.2 ± 0.1	1.52 ± 0.08	2.15 ± 0.05	23.4 ± 0.08	0.54 ± 0.01
2a	2.95 ± 0.04	5.76 ± 0.08	1.63 ± 0.08	1.95 ± 0.04	31.6 ± 0.8	0.29 ± 0.01
2b	4.6 ± 0.2	9.1 ± 0.3	2.5 ± 0.3	2.0 ± 0.1	38 ± 1	0.31 ± 0.01
2c	4.2 ± 0.1	7.8 ± 0.3	2.2 ± 0.3	1.9 ± 0.1	34 ± 1	0.27 ± 0.01
2d	2.59 ± 0.03	5.70 ± 0.05	1.25 ± 0.03	2.20 ± 0.03	33.0 ± 0.6	0.48 ± 0.01
2e	3.66 ± 0.07	9.1 ± 0.2	2.6 ± 0.2	2.49 ± 0.07	38 ± 1	0.33 ± 0.01

to, or even higher than, those of the other polymers, as shown in Table 2. However, the weight-averaged absolute molecular weight, obtained from the results of the true calibration curves of Figure 3 (Table 3), is considerably lower since the molecules elute in SEC according to their hydrodynamic volume and not to their molecular weight.

Figure 5 shows the root-mean-square radius of gyration, $\langle s^2 \rangle^{1/2}$, versus the elution volume for the polyphosphazenes; the signals from the differential refractive index detector are also shown. The accuracy in the determination of the radius of gyration decreases for low molecular weights (elution volumes higher than 12 mL), since the size of the polymer must be larger than $\lambda/20$ in order to observe the angular dependence of the scattered light intensity.¹⁶ The values of $\log \langle s^2 \rangle^{1/2}$ versus volume are linear for the polymers only in the region of low volumes, i.e., high molecular weights. This behavior has been described for other polyphosphazenes.^{17,18} Values of the root-mean-square radii of gyration calculated from the z -averaged mean-square radius of each slice of the chromatogram using ASTRA software are shown in the sixth column of Table 3.

The behavior of the polymer through a very large range of molecular weights can be deduced from the comparison of molecular weight and radius of gyration for the slices of the SEC chromatogram¹⁹ of each sample. Figure 6 shows the log–log plot of the radius of gyration versus molecular weight, which is the scaling law, $\langle s^2 \rangle^{1/2}$

$= QM^q$, obtained for the polymer samples.²⁰ It can be noticed that at high molecular weights the plots are linear and deviate from linearity in the region of lower molecular weights. This behavior is a consequence of the molecular weight and dimension versus elution volume results implicit in Figures 4 and 5 and has been found for other polyphosphazenes.¹⁸ It has also been observed for polystyrene aggregates¹⁵ and for cylindrical macromolecules with high chain stiffness.^{21,22} The reason for this anomalous elution behavior has been explained^{21,22} by the existence of a small fraction of very large molecules that are retarded in the column. At small elution volumes, the molecules elute according to their hydrodynamic volume (normal SEC) whereas at higher elution volumes the normally eluting small molecules coelute with the retarded large molecules. The mechanism of the retardation is not clear although it seems that molecular architecture plays an important role.²²

The slope of the log–log plot of the radius of gyration versus molecular weight provides the q coefficient from which information about the shape of the chain can be deduced.²⁰ Values of $0.5 \leq q \leq 0.6$ are predicted for random-coil chains, from polymers in θ conditions (0.5) to polymers in very good solvents. On the other hand, values of $1/3$ and 1 are expected for spherical and rigid-rod-like molecules, respectively. The values of the q coefficient for the linear part of the plots of the radius of gyration versus molecular weight at low elution

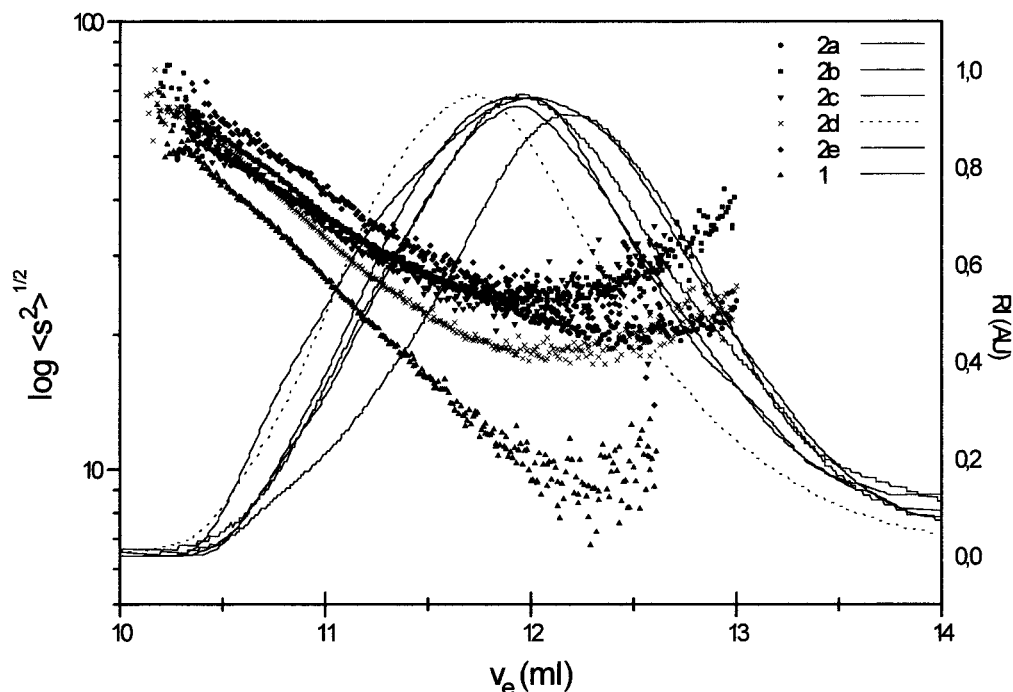


Figure 5. Logarithm of root-mean-square radius of gyration versus elution volume for polymers 1, 2a, 2b, 2c, 2d, and 2e. The corresponding DRI signals are also shown.

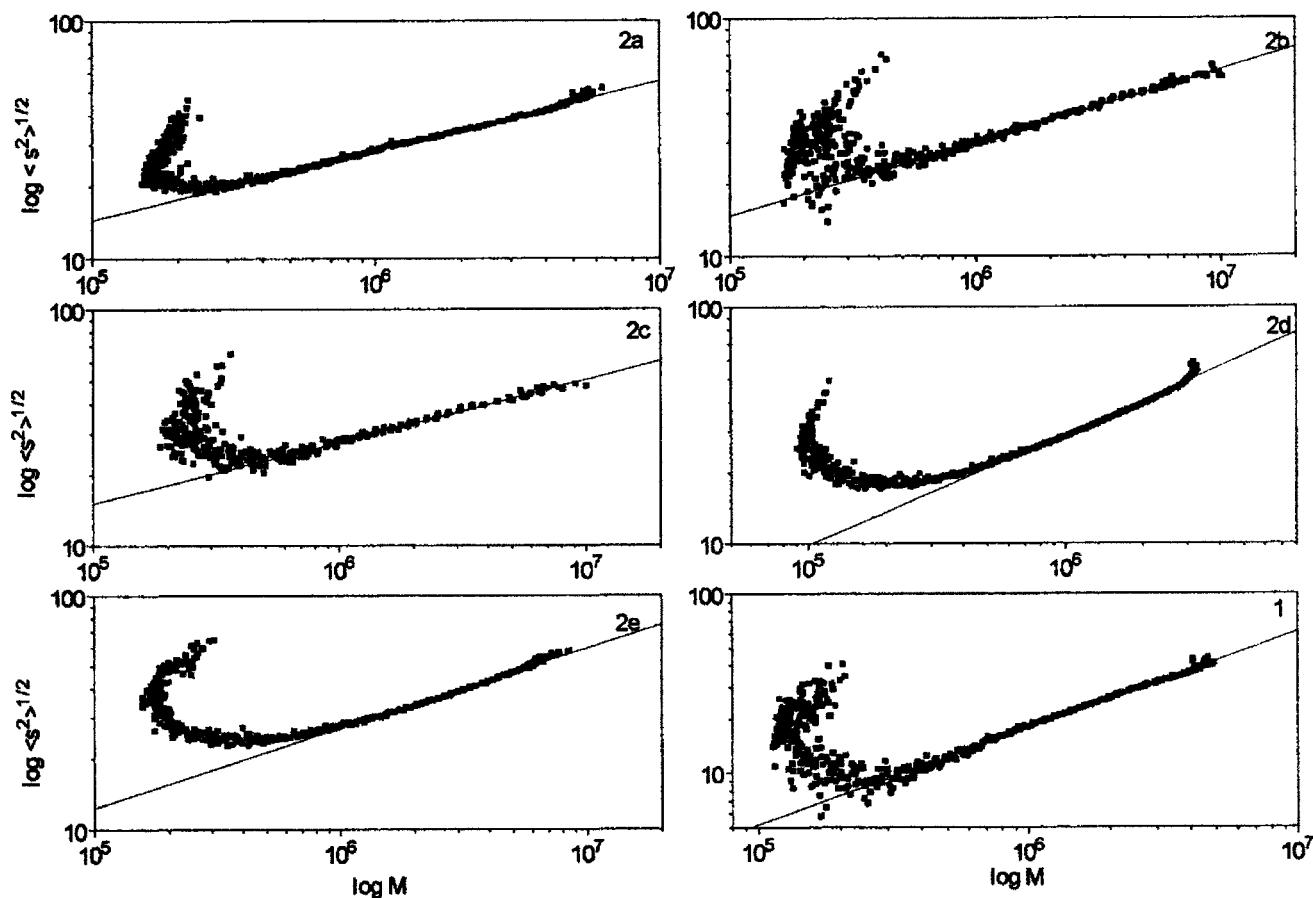


Figure 6. Log-log plot of root-mean-square radius of gyration versus molecular weight for the polymers in the whole range of molecular weights.

volumes (i.e., high molecular weights) are shown in the last column of Table 3. As stated above, curvature appears in the plots if the range is expanded toward higher elution volumes. The values of the q parameter show that polymers 2a, 2b, 2c, and 2e have a $q \sim 0.3$,

which might indicate that the polymers aggregate in a globular shape, whereas polymer 2d has $q = 0.48$ and thus seems to be in random coil close to θ conditions. On the other hand, homopolymer 1 behaves as a random coil in a good solvent ($q = 0.54$).

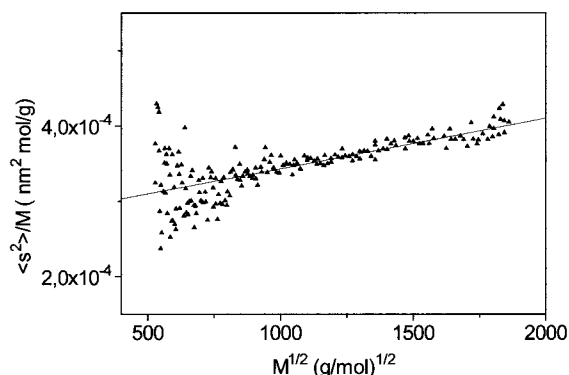


Figure 7. Fixman extrapolations for the polymer 1.

Unperturbed dimensions²³ can be evaluated from SEC-MALLS measurements of dimensions of the polymers as a function of molecular weight in a good solvent, using several extrapolation procedures.^{18,19} Two different extrapolation procedures have been used here for the homopolymer 1. The first one, due to Fixman,²⁴ is defined in eq 1 and provides $\langle s^2 \rangle_0 / M$ as the intercept:

$$\frac{\langle s^2 \rangle}{M} = \frac{\langle s^2 \rangle_0}{M} + 0.0299B \left(\frac{\langle s^2 \rangle_0}{M} \right)^{-1/2} M^{1/2} \quad (1)$$

The other procedure used is similar to the extrapolation of Stockmayer–Fixman²⁵ for viscosity measurements (eq 2):

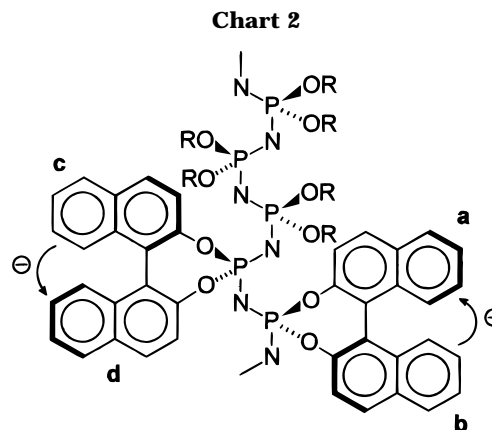
$$\left(\frac{\langle s^2 \rangle}{M} \right)^{3/2} = \left(\frac{\langle s^2 \rangle_0}{M} \right)^{3/2} (1 + CM^{1/2}) \quad (2)$$

The Fixman plot of polymer 1 is represented in Figure 7. The Stockmayer–Fixman plot is similar. The derived values of $\langle s^2 \rangle_0 / M$, in nm² mol g⁻¹, for both extrapolations are $(2.84 \pm 0.05) \times 10^{-4}$ and $(2.9 \pm 0.1) \times 10^{-4}$, respectively. It is worth noting that, despite the dispersion of the points, the errors in the intercepts are not too large and, as expected, there is good accord between the two extrapolations. The characteristic ratio C_n can be calculated from the extrapolated values of $\langle s^2 \rangle_0 / M$ as²³

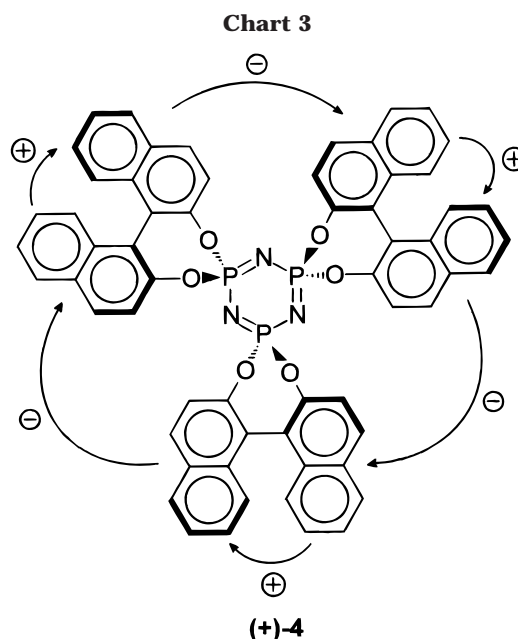
$$C_n = \frac{\langle r \rangle_0}{nl^2} = \frac{6M_0 \langle s^2 \rangle_0}{2l^2 M} \quad (3)$$

where n is the number of P–N bonds of length $l = 0.152$ nm, $\langle r \rangle_0$ the unperturbed value of the mean-square end-to-end distance, and M_0 the molecular weight of the repetitive unit. The $\langle r^2 \rangle_0 = 6\langle s^2 \rangle_0$ relationship valid for flexible chains has been used in the above equation. The value obtained $C_n = 14$ is in the range obtained for other polyphosphazenes,²⁶ and its high value indicates a fairly extended chain.

The specific rotation $[\alpha]_D$ of polymers 2, measured at $c = 1$ near 20 °C in CHCl₃, was, as expected,² opposite in sign to that of the binaphthol used (measured in THF) and increased with the number of binaphthoxy units, varying from -59 ($x = 0.08$) to -149 ($x = 0.7$) (see Table 2). The data seemed to suggest that $[\alpha]_D$ increases very fast upon the incorporation of a few quiral units, then the increase is much slower from 0.2 to 0.7, and finally it increases rapidly again from 0.7, reaching the value -214 corresponding to the homopolymer 1. The $[\alpha]_D$ values were almost constant with the concentration, changing only a few units from $c = 1$ to $c = 0.2$. This



(-)-1 in the (TC)_n backbone conformation



behavior is difficult to interpret because the presence of phenoxy groups in the polymers introduces changes in their chemical composition that affect the overall specific rotation. However, it is in accord with the possibility that, in all cases, there are contributions originating in the presence of helicoidal conformations that allow some level of interaction between contiguous chiral units.² These contributions are likely to increase with the number of binaphthoxy groups along the chain due to the increase of interacting diads and triads of units.²⁷ This conclusion is not in contradiction with the globular or random-coil structures discussed above since locally helical segments in the chain would be sufficient to allow the interaction between the chiral units. Moreover, the presence of those segments would lead to complex chain structures that would cause both the anomalous elution effect and the high unperturbed dimensions obtained for homopolymer 1 and other similar polyphosphazenes.¹⁸

To obtain further information on the stereochemistry of these polymers, CD spectra of the homopolymers (+)- and (-)-1² and the copolymers 2a–e were recorded. In addition, the CD spectra of (+)- and (-)-binaphthol and that of the cyclic trimer 4² (Chart 3) were measured for comparison with those of the homopolymers.

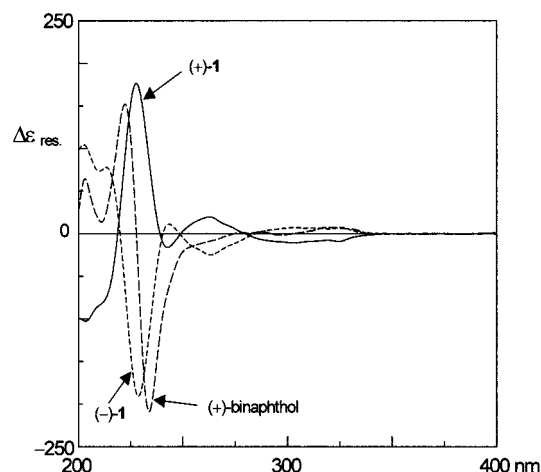


Figure 8. CD spectra of the enantiomeric homopolymers **1** and (*R*)-(+)-binaphthol in CH_3CN . The reported $\Delta\epsilon$ are per residue.

The complex CD spectra of the enantiomeric homopolymers **1** (Figure 8) showed, as expected, opposite Cotton effects at the same wavelengths and with almost the same intensities. Furthermore, it can be observed that homopolymers (*-*)-**1** and (+)-**1** exhibited strong split CD curves with the first negative/positive Cotton effect located at 229 nm ($\Delta\epsilon_{\text{res}}$ -191/+177) and the positive/negative second Cotton effect at 213 nm ($\Delta\epsilon_{\text{res}}$ +78/-80), respectively, as a consequence of the exciton coupling interaction between the $^1\text{B}_b$ transition of the naphthalene chromophores, which is polarized along the long axis of the chromophore.²⁸ The reported $\Delta\epsilon$ values for these homopolymers are per residue; namely, they were calculated using the molecular weight of the residue, to compare them with those of (+)-binaphthol, which showed a split CD curve with the first negative Cotton effect located at 234 nm ($\Delta\epsilon$ -209) and the positive second Cotton effect at 222 nm ($\Delta\epsilon$ +152).

According to the exciton chirality method,²⁸ the sign of the split Cotton effects depends on the absolute disposition of the chromophores. Therefore, the split Cotton effects observed for compounds (*-*)-**1** and (+)-**1** were in agreement with the absolute configuration of the (+)- and (*-*)-binaphthol used respectively in their preparation.

CD spectral comparison shows that the intensities of the first exciton Cotton effects of the homopolymers are slightly smaller than that of binaphthol. Since it is well-known that the exciton chirality depends on the interchromophoric distance and the dihedral angle between the electric transition moment of the chromophores,²⁸ the observed CD spectra of homopolymers **1** are mainly due to the exciton coupling interaction between naphthalene chromophores at each binaphthoxy unit. In addition, the most likely backbone conformation $[\text{TC}]_n$ ([trans, cis]_n) for this type of polymers²⁹ allows us to explain the decrease observed in the CD spectra of the polymers (+)- and (*-*)-**1** with respect to that of binaphthol by observing the sign of the pairwise interactions present. Thus, for compound (*-*)-**1** (Chart 2), besides the very strong negative interactions between chromophores at the same binaphthoxy residue (**a/b** and **c/d**), other interactions between chromophores at continuous residues were observed: two positive interactions, between chromophores **b** and **c**, and **a** and **c**, as well as one negative interaction between the chromophores **b** and **d**. These weak interactions, due to higher interchro-

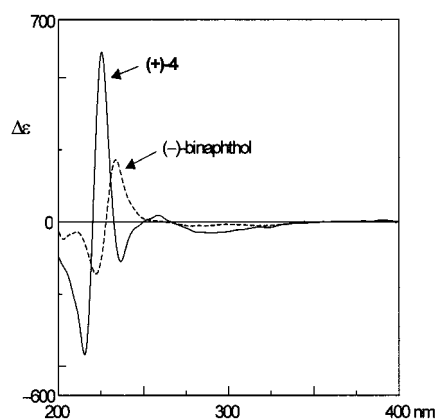


Figure 9. CD spectra of the cyclic trimer (+)-**4** and (*S*)-(*-*)-binaphthol in CH_3CN .

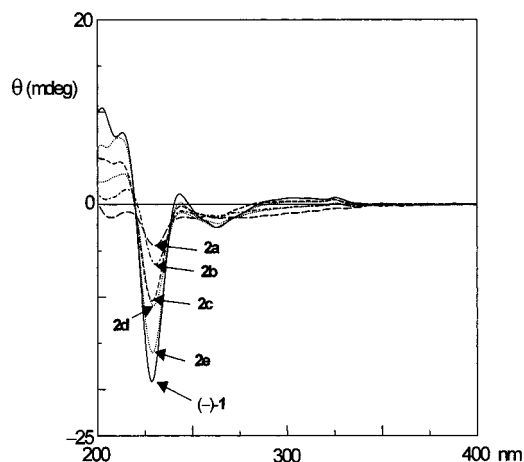


Figure 10. CD spectra of the homopolymer (*-*)-**1** and copolymers (*-*)-**2a-e**. All these spectra were normalized to a concentration of 1×10^{-3} mg/mL (CH_3CN).

morphic distances and small dihedral angles of the electric transition moment of the chromophores, together with the high degree of parallelism between chromophores located at 1,3 residues, make a net positive contribution to the CD spectra of the homopolymers **1**, therefore explaining their slightly smaller CD intensities.

CD spectral comparison of the cyclic trimer (+)-**4** (*A* value +1047) and (*-*)-binaphthol (*A* value +361) revealed (Figure 9) for the former an intensity only 2.90 times higher than that of binaphthol. The pairwise interactions involved in compound (+)-**4** are shown in Chart 3; thus, there are three positive exciton coupling interactions, between naphthalene chromophores at the same residue, and three negative interactions, between chromophores located at different residues. Therefore, to explain the small decrease observed in the CD spectrum of the cyclic trimer (+)-**4** with respect to binaphthol, as occurred with the homopolymers, the contribution of these negative exciton coupling interactions to the total spectrum must be small. This fact confirms our above-mentioned interpretation of the CD spectra of homopolymers **1**.

The complex CD spectra of the copolymers (*-*)-**2a-e** together with that of the homopolymer (*-*)-**1** are shown in Figure 10. A general decrease can be observed in the intensity of the first and second exciton Cotton effects from (*-*)-**1** to **2a**, in good agreement with the amount of binaphthoxy groups present in the copolymers.

Acknowledgment. We thank Spanish Dirección General de Investigación Científica y Técnica (D.G.I.C.Y.T.), Projects PB97-1276 and PB97-0778, and the Fomento de la Investigación Científica y Técnica (FICYT), Project. PB-MAT8-02.

References and Notes

- (1) Manners, I. *Angew. Chem., Int. Ed. Engl.* **1996**, *35*, 1602.
- (2) Carriedo, G. A.; García Alonso, F. J.; González, P. A.; García Alvarez, J. L. *Macromolecules* **1998**, *31*, 3189.
- (3) Sulkowski, W.; Sulkowska, A.; Kireev, V. *J. Mol. Struct.* **1997**, *410-411*, 241.
- (4) Bao, J.; Wulff, W. D.; Dominy, J. B.; Fumo, M. J.; Grant, E. B.; Rob, A. C.; Whitcomb, M. C.; Yeung, S.-M.; Ostrander, R. L.; Rheingold, A. L. *J. Am. Chem. Soc.* **1996**, *118*, 3392.
- (5) Sogah, G. D. Y.; Cram, D. J. *J. Am. Chem. Soc.* **1979**, *101*, 3035.
- (6) Huang, W.-S.; Hu, Q.-S.; Zheng, X.-F.; Anderson, J.; Pu, L. *J. Am. Chem. Soc.* **1997**, *119*, 4313.
- (7) Qian, P.; Matsuda, M.; Miyashita, T. *J. Am. Chem. Soc.* **1993**, *115*, 5624.
- (8) Mujumdar, A. N.; Young, S. G.; Merker, R. L.; Magill, J. H. *Macromolecules* **1990**, *23*, 14.
- (9) Hu, Q.-S.; Vitharana, D.; Pu, L. *Tetrahedron: Asymmetry* **1995**, *6*, 2123.
- (10) Moore, J. A.; Kaur, S. *Macromolecules* **1997**, *30*, 3428.
- (11) Mark, J. E.; Allcock, H. R.; West, R. *Inorganic Polymers*; Prentice Hall: Englewood Cliffs, NJ, 1992; p 89.
- (12) Gómez, M. A.; Marco, C.; Gómez Fatou, J. M.; Carriedo, G. A.; García Alonso, F. J.; Gómez Elipe, P. *Eur. Polym. J.* **1996**, *32*, 717.
- (13) Singler, R. E.; Hagnauer, G. L.; Schneider, N. S.; LaLiberte, B. R.; Sacher, R. E.; Matton, R. W. *J. Polym. Sci., Polym. Chem. Ed.* **1974**, *12*, 433.
- (14) Brandrup, J.; Immergut, E. H., Eds. *Polymer Handbook*, 3rd ed.; Wiley: New York, 1989; Chapter VII.
- (15) Wyatt, P. J. *Anal. Chim. Acta* **1993**, *272*, 1.
- (16) Huglin, M. B., Ed. *Light Scattering from Polymer Solutions*; Academic Press: London, 1972; Chapter 7.
- (17) Mourey, T. H.; Miller, S. M.; Ferrar, W. T.; Molaire, T. R. *Macromolecules* **1989**, *22*, 4286.
- (18) Búrdalo, J.; Tarazona, M. P.; Carriedo, G. A.; García Alonso, F. J.; González, P. A. *Polymer* **1999**, *40*, 4251.
- (19) Búrdalo, J.; Medrano, R.; Saiz, E.; Tarazona, M. P. *Polymer* **1999**, *40*, 18.
- (20) De Gennes, P. G. *Scaling Concepts in Polymer Physics*; Cornell University Press: Ithaca, NY, 1979.
- (21) Percec, V.; Ahn, C. H.; Cho, W. D.; Jamieson, A. M.; Kim, J.; Leman, T.; Schmidt, M.; Gerle, M.; Möller, M.; Prokhorova, S. A.; Sheiko, S. S.; Cheng, S. Z. D.; Zhang, A.; Ungar, G.; Yearley, D. J. P. *J. Am. Chem. Soc.* **1998**, *120*, 8619.
- (22) Gerle, M.; Fischer, K.; Roos, S.; Müller, A. H. E.; Schmidt, M. *Macromolecules* **1999**, *32*, 2629.
- (23) Flory, P. J. *Statistical Mechanics of Chain Molecules*; Wiley: New York, 1969.
- (24) Fixman, M. *J. Chem. Phys.* **1955**, *23*, 1656.
- (25) Stockmayer, W. H.; Fixman, M. *J. Polym. Sci.* **1963**, *C1*, 137.
- (26) Tarazona, M. P. *Polymer* **1994**, *35*, 819.
- (27) Obata, M.; Kakuchi, T.; Yokota, K. *Macromolecules* **1997**, *30*, 348.
- (28) (a) Harada, N.; Nakanishi, K. *Circular Dichroic Spectroscopy Exciton Coupling in Organic Stereochemistry*; University Science Books: CA, 1983. (b) Nakanishi, K.; Berova, N. In *The Exciton Chirality Method in Circular Dichroism, Principles and Applications*; Nakanishi, K., Berova, N., Woody, R. W., Eds.; VCH Publishers: New York, 1994.
- (29) Caminiti, R.; Gleria, M.; Lipkowitz, K. B.; Lombardo, G. M.; Pappalardo, G. C. *Chem. Mater.* **1999**, *11*, 1492.

MA991904B